Available online at www.sciencedirect.com
SCIENCE DIRECT®
Journal of Computational Physics 201 (2004) 109–118
JOURNAL OF COMPUTATIONAL PHYSICS
www.elsevier.com/locate/jcp

Isotropic finite-differences

Anand Kumar *

CSIR Centre for Mathematical Modelling and Computer Simulation, Belur, Bangalore 560037, India

Received 1 October 2003; received in revised form 24 March 2004; accepted 10 May 2004
Available online 10 June 2004

Abstract

New finite-differences, called isotropic finite-differences, where the lowest order error terms are without any directional bias, are proposed. An accurate simulation of 6-fold symmetric dendritic solidification is presented using a numerical scheme based on these finite-differences.

Keywords: Directional bias; Dendritic solidification; Phase-field simulation; Grid refinement

1. Introduction

Various methods, e.g. compact schemes, Padé approximation, etc., have been followed to improve the accuracy of the numerical simulation of partial differential equations (PDEs). These methods are generally based on constructing higher order schemes. In the present work, we consider another aspect of the numerical simulation, namely, the isotropy. In order to preserve the isotropy (or anisotropy) in the problem being simulated the numerical scheme must not add its own anisotropy to the simulation. The numerical scheme therefore should be isotropic (a numerical scheme is defined to be isotropic if it does not have a directional preference). The notion of isotropy of the numerical scheme can be relevant to many simulations, e.g. simulation of microstructural evolution, turbulence, etc.

When conventional finite-differences are used to discretise a PDE they introduce an anisotropy into the numerical scheme. This anisotropy into the scheme comes from the directional bias of the error terms in the discretisation. We propose new finite-differences, called isotropic finite-differences, where the lowest order error terms are without any directional bias. (Due to discretisation a continuous problem is reduced to a finite dimensional discrete problem. The discretisation therefore may achieve only a limited isotropy.) A method to derive these finite-differences is given, and various formulae are obtained in two-dimension.

Dendritic solidification, a typical microstructural evolution problem, is a well studied topic [1–5]. A simulation of 6-fold symmetric dendritic solidification is considered here to show the effect of numerical

* Tel.: +91-80-2505-1930; fax: +91-80-2522-0392.
E-mail address: kumar@cmmacs.ernet.in (A. Kumar).

0021-9991/$ - see front matter
doi:10.1016/j.jcp.2004.05.005

anisotropy. Since the physical symmetry of the problem must be preserved in the simulation, we accordingly look for the 6-fold symmetry of the simulated solidification front. It is shown that when a numerical scheme based on the directionally biased conventional finite-differences is used the 6-fold symmetry is not well preserved in the simulation. On the other hand, using a scheme based on isotropic finite-differences, the symmetry in the simulation is found to be well preserved. We note that improvement in the capturing of the physical symmetry in the simulation is achieved here by making the numerical scheme isotropic, the order of accuracy of the two schemes being the same.

The rest of the paper is organised as follows. Section 2 describes how the directional bias arises in a numerical scheme, isotropic finite-difference formulae are derived in Section 3, the simulation of dendritic solidification is considered in Section 4, and lastly, Section 5 gives the conclusions. Isotropic finite-difference formulae in three-dimension are given in Appendix A.

2. Anatomy of a numerical discretisation

Let us consider a numerical scheme for the solution of the Laplace equation

$$\psi_{xx} + \psi_{yy} = 0, \tag{1}$$

where the subscripts denote the partial derivatives. Discretising the derivatives in the above PDE by the conventional central differences, $\psi_{xx} = (\psi_{i+1,j} - 2\psi_{i,j} + \psi_{i-1,j})/h^2$, and $\psi_{yy} = (\psi_{i,j+1} - 2\psi_{i,j} + \psi_{i,j-1})/h^2$, where h is the step size, we obtain

$$\frac{1}{h^2}\left(\psi_{i+1,j} + \psi_{i-1,j} + \psi_{i,j+1} + \psi_{i,j-1} - 4\psi_{i,j}\right) = 0. \tag{2}$$

The discrete system (2), along with appropriate boundary conditions, are solved to obtain the numerical solution of (1).

From a Taylor expansion, (2) represents

$$\nabla^2\psi + \frac{h^2}{12}\left(\psi_{xxxx} + \psi_{yyyy}\right) + \mathcal{O}(h^4) = 0. \tag{3}$$

Eq. (3) is referred to as the modified PDE, the equivalent PDE one solves to obtain the numerical solution of (1). Eq. (3) has a directional bias, which comes from the error terms. This anisotropy in the numerical scheme would be present no matter how so ever small is h.

3. Isotropic finite-differences

We propose new finite-differences where the lowest order error terms are without any directional bias. Various isotropic finite difference formulae are obtained in two-dimension. These formulae in two-dimension, unlike conventional finite-differences, involve various points of the nine-point stencil. A simulation is presented later (Section 4) to test these finite-differences.

3.1. First derivative

Conventional finite difference formula for the first derivative is

$$(\psi_{x_C})_{i,j} = \frac{1}{2h}\left(\psi_{i+1,j} - \psi_{i-1,j}\right). \tag{4}$$

The above formula involves only points along x-direction. From a Taylor expansion, Eq. (4), to $\mathcal{O}(h^2)$, is written as

$$(\psi_{x_C})_{i,j} = \left(1 + \frac{h^2}{6}\delta_{xx}\right)(\psi_x)_{i,j}. \tag{5}$$

The anisotropy in a numerical scheme using the above finite-difference can arise from the term of $\mathcal{O}(h^2)$.

We propose to obtain the isotropic finite difference of ψ_x from

$$(\psi_{x_I})_{i,j} = \left(1 + \frac{h^2}{6}\nabla^2\right)(\psi_x)_{i,j}. \tag{6}$$

Note the similarity of the Eq. (6) to Eq. (5). Eq. (6), to $\mathcal{O}(h^2)$, can be written as

$$(\psi_{x_I})_{i,j} = \left(1 + \frac{h^2}{6}\delta_{yy}\right)\left(1 + \frac{h^2}{6}\delta_{xx}\right)(\psi_x)_{i,j} = \left(1 + \frac{h^2}{6}\delta_{yy}\right)(\psi_{x_C})_{i,j}.$$

The above in expanded form, to $\mathcal{O}(h^2)$, is

$$(\psi_{x_I})_{i,j} = \frac{1}{2h}\left[\frac{1}{6}\left(\psi_{i+1,j+1} - \psi_{i-1,j+1}\right) + \frac{4}{6}\left(\psi_{i+1,j} - \psi_{i-1,j}\right) + \frac{1}{6}\left(\psi_{i+1,j-1} - \psi_{i-1,j-1}\right)\right]. \tag{7}$$

Eq. (7) is a $\mathcal{O}(h^2)$ accurate discretisation of ψ_x. Unlike conventional finite-differences, it is seen to involve points not only along the x-direction, but also along the y-direction.

The Taylor expansion of (7), up to $\mathcal{O}(h^2)$, is given by (6). The leading order error term in (7) involves only the Laplacian. We have referred (7) to be the isotropic finite-difference of ψ_x, based on the notion that the leading order error term has no directional preference. A numerical example is presented later (Section 4) to test these so-derived isotropic finite-differences.

3.2. An example

Consider the finite differencing of the terms

$$a\psi_x + b\psi_y,$$

which arise in many convection problems. The conventional finite-difference of the above is equivalent to

$$(a\psi_x + b\psi_y)_C = a\psi_x + b\psi_y + \frac{h^2}{6}(a\psi_{xxx} + b\psi_{yyy})$$

and the isotropic finite-difference is equivalent to

$$(a\psi_x + b\psi_y)_I = \left(1 + \frac{h^2}{6}\nabla^2\right)(a\psi_x + b\psi_y).$$

As seen from the above Taylor expansion, the isotropic discretisation preserves the direction of propagation to $\mathcal{O}(h^2)$.

3.3. Second derivative

Conventional finite-difference of the second derivative is given by

$$(\psi_{xx_C})_{i,j} = \frac{1}{h^2}\left(\psi_{i+1,j} - 2\psi_{i,j} + \psi_{i-1,j}\right),$$

which from a Taylor expansion is equivalent to

$$(\psi_{xx_C})_{i,j} = \left(1 + \frac{h^2}{12}\partial_{xx}\right)(\psi_{xx})_{i,j}.$$

The isotropic finite-difference of ψ_{xx} is obtained from

$$(\psi_{xx_I})_{i,j} = \left(1 + \frac{h^2}{12}\nabla^2\right)(\psi_{xx})_{i,j}. \tag{8}$$

The above, to $\mathcal{O}(h^2)$, is written as

$$(\psi_{xx_I})_{i,j} = \left(1 + \frac{h^2}{12}\partial_{yy}\right)(\psi_{xx_C})_{i,j},$$

which gives

$$(\psi_{xx_I})_{i,j} = \frac{1}{h^2}\left[\frac{1}{12}\left(\psi_{i+1,j+1} - 2\psi_{i,j+1} + \psi_{i-1,j+1}\right) + \frac{10}{12}\left(\psi_{i+1,j} - 2\psi_{i,j} + \psi_{i-1,j}\right) + \frac{1}{12}\left(\psi_{i+1,j-1} - 2\psi_{i,j-1} + \psi_{i-1,j-1}\right)\right]. \tag{9}$$

3.4. Cross derivative

The conventional evaluation of the derivative ψ_{xy} is given by

$$(\psi_{xy_C})_{i,j} = \frac{1}{4h^2}\left(\psi_{i+1,j+1} - \psi_{i-1,j+1} - \psi_{i+1,j-1} + \psi_{i-1,j-1}\right).$$

A Taylor expansion of the above gives,

$$(\psi_{xy_C})_{i,j} = \left(1 + \frac{h^2}{6}\nabla^2\right)(\psi_{xy})_{i,j}.$$

The derivative ψ_{xy_C} is therefore isotropic, and hence

$$(\psi_{xy_I})_{i,j} = (\psi_{xy_C})_{i,j}. \tag{10}$$

3.5. Laplacian

The isotropic discretisation of the Laplacian is obtained from

$$\nabla^2_I\psi = (\psi_{xx})_I + (\psi_{yy})_I. \tag{11}$$

Substituting from Eq. (9) we get

$$(\nabla^2_I\psi)_{i,j} = \frac{1}{6h^2}\left(4\sum_{NN}\psi + \sum_{NNN}\psi - 20\psi\right)_{i,j}, \tag{12}$$

where *NN* in the first summation refers to nearest-neighbour points that lie along the axes, and *NNN* in the second summation to next-nearest-neighbour points that lie along the diagonals.

The discretisation (12) has been considered before [6]. It has also been used in [7] where it is stated to be rotationally invariant. It may be noted that the discretisation (12) is obtained here by isotropic finite-differencing the individual terms in the Laplacian.

Isotropic finite-differences, due to a larger foot-print, will in general lead to a more stable numerical scheme. Consider, e.g. the heat conduction equation

$$\frac{\partial u}{\partial t} = \nabla^2 u.$$

Stability criterion for the above equation using the conventional central differences is known to be $\Delta t/h^2 \leqslant 1/4$, where Δt is the step size in t. When Eq. (12), the isotropic discretisation of the Laplacian, is used, the stability criterion becomes $\Delta t/h^2 \leqslant 3/8$. The stability is thus enhanced using the isotropic discretisation.

4. Dendritic solidification

We present a simulation of 6-fold symmetric dendritic solidification to show the effect of anisotropy in the numerical scheme on the simulation, and to test the isotropic finite-differences. We look for the 6-fold symmetry in the simulated solidification pattern. A feature of the problem is the intense release of energy (latent heat) at the solidification front.

4.1. Phase-field equations

The phase-field equations for dendritic solidification are:

$$\frac{\partial u}{\partial t} = D\nabla^2 u + \frac{1}{2}\frac{\partial \phi}{\partial t}, \tag{13}$$

$$\tau(\theta)\frac{\partial \phi}{\partial t} = \nabla \cdot \left[W_0^2 A^2(\theta)\nabla\phi\right] - \frac{\partial F(\phi, \lambda u)}{\partial \phi} - \frac{\partial}{\partial x}\left(W_0^2 A(\theta)A'(\theta)\phi_y\right) + \frac{\partial}{\partial y}\left(W_0^2 A(\theta)A'(\theta)\phi_x\right), \tag{14}$$

where u is the dimensionless temperature, and ϕ the order parameter. The above equations are obtained from the equations given in [4] by expressing the direction in terms of θ, where $\theta = \tan^{-1}(\phi_y/\phi_x)$. $A(\theta)$ for k-fold symmetry ($k = 6$ for 6-fold symmetry) is given by $A(\theta) = 1 + \varepsilon\cos(k\theta)$, where ε is the strength of anisotropy, and $\tau(\theta) = \tau_0 A^2(\theta)$. According to Model 2 of [4], we take $\partial F/\partial\phi = -\phi(1-\phi^2) + \lambda u(1-\phi^2)^2$, $a_1 = 1.25/\sqrt{2}$, and $a_2 = 0.64$. Further, $\lambda = W_0 a_1/d_0$, $\tau_0 = W_0^3 a_1 a_2/(d_0 D) + W_0^2\beta_0/d_0$. We take $\varepsilon = 0.05$, $\beta_0 = 0$, $W_0 = 1$, $D = 2$, and $d_0 = 0.5$.

4.2. Computational schemes

Two schemes, one based on the conventional central differences, and the other on the isotropic finite-differences are considered. The derivatives in the above equations are discretised using the conventional central differences in the scheme referred to as the conventional scheme, and using the isotropic finite-differences in the scheme referred to as the isotropic scheme.

The term $\partial\phi/\partial t$, computed from (14), is used as the source term in (13). In (14) a small dissipative term is added, and subtracted from its source term. The equations are integrated in time using an alternating-direction implicit (ADI) scheme, described in Appendix B.

4.3. Results and discussion

At $t = 0$, a small circular seed (solid) in an undercooled liquid is taken, i.e., $u = 0$, $\phi = 1$ for radius $r < r_0$, and $u = -\Delta\{1 - e^{-(r-r_0)}\}$, $\phi = -1$ for $r \geqslant r_0$, where r_0 is the radius of the seed, and Δ is the undercooling. We take $\Delta = 0.8$, and $r_0 = 5$.

A computational domain of 200×200 is taken for $0 \leqslant t \leqslant 150$, which is progressively increased to 320×320 for $150 \leqslant t \leqslant 250$, and to 480×480 for $250 \leqslant t \leqslant 400$.

Solidification front ($\phi = 0$) obtained using the directionally biased conventional scheme on a grid with step size $h = 0.4$ is shown in Fig. 1. The solidification front is seen to be symmetric in the two coordinates. (Note that a 4-fold symmetric solidification normally will not reveal the anisotropy in the numerical scheme.) We assess the 6-fold symmetry of the simulated solidification front from the computed angle of the second petal, counting the petals in the counter-clockwise direction, starting with the petal along the x-axis. This angle is given in Table 1 for various t. This angle for the 6-fold symmetry should be 60°. The computed angle of the second petal is seen to deteriorate with time. It is thus not well preserved in the simulation.

We also investigate grid refinement for the improvement of the simulation. Computation on a fine grid with $h = 0.2$ is performed, taking about 900 h of CPU time on SGI Origin 3400, the final computational grid being 2400×2400. The computed angle of the second solidification petal is also given in Table 1. Some improvements in the symmetry can be seen for small time, but it deteriorates with increasing time. Improvements in the computed angle for small time may suggest that a sufficiently fine grid can give a solution of desired accuracy even though the numerical scheme is anisotropic; although we may achieve this at a great computational cost.

Simulations using the scheme based on isotropic finite-differences are also carried out on the two grids ($h = 0.4$ and 0.2). Table 1 also gives the computed angle of the second petal in these simulations, which is found to be remarkably well captured. A comparison of the solidification front given by the two schemes is shown in Fig. 2, where the effect of numerical anisotropy in the conventional scheme simulation can be seen. The isotropic scheme computation on the fine grid takes about 1000 h of CPU time.

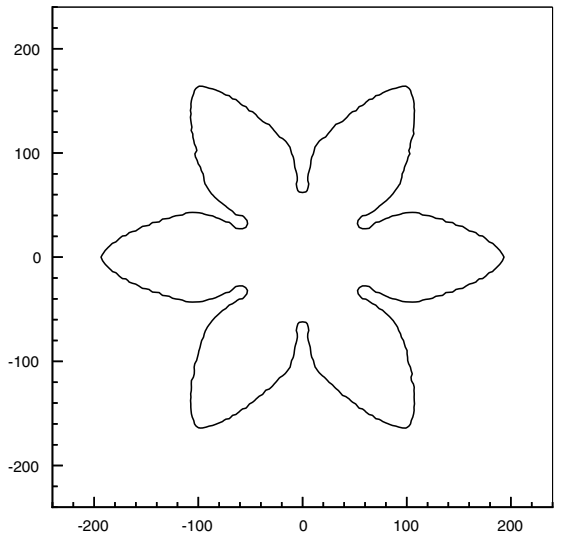

Fig. 1. Solidification front obtained using the conventional scheme on the grid with $h = 0.4$, and $t = 400$.

Table 1
Computed angle of the second petal given by (a) the conventional scheme, and by (b) the isotropic scheme

h	t		
	150	250	400
(a) Conventional scheme			
0.4	58.94°	58.45°	58.10°
0.2	59.18°	58.97°	57.66°
(b) Isotropic scheme			
0.4	60.04°	59.75°	59.77°
0.2	60.01°	59.93°	60.16°

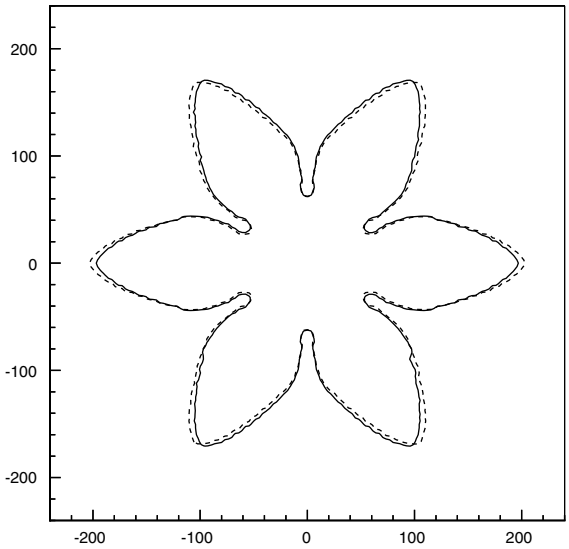

Fig. 2. Comparison of the solidification fronts on the fine grid ($h = 0.2$) obtained using the isotropic scheme, ——, and the conventional scheme, - - - - -. $t = 400$.

5. Conclusions

A simulation of 6-fold dendritic solidification is presented to show that due to the anisotropy in the numerical scheme the physical symmetry of the problem is not well preserved in the simulation. A grid refinement study is also presented.

We have proposed new finite-differences, called isotropic finite-differences. A scheme based on isotropic finite-differences is also used for the above simulation, where the 6-fold symmetry is found to be easily captured. An isotropic numerical scheme therefore may be necessary to capture the physical properties of the problem in the simulation.

Appendix A. Isotropic finite-differences in three-dimension

The conventional finite difference of ψ_x is

$$(\psi_{x_C})_{i,j,k} = \frac{1}{2h}(\psi_{i+1,j,k} - \psi_{i-1,j,k}),$$

which to $\mathcal{O}(h^2)$ gives

$$(\psi_{x_C})_{i,j,k} = \left(1 + \frac{h^2}{6}\eth_{xx}\right)(\psi_x)_{i,j,k}.$$

Isotropic finite difference of ψ_x is obtained from

$$(\psi_{x_I})_{i,j,k} = \left(1 + \frac{h^2}{6}\nabla^2\right)(\psi_x)_{i,j,k}.$$

We express the above, to $\mathcal{O}(h^2)$, as

$$(\psi_{x_I})_{i,j,k} = \left(1 + \frac{h^2}{6}\eth_{zz}\right)\left(1 + \frac{h^2}{6}\eth_{yy}\right)(\psi_{x_C})_{i,j,k}.$$

The above in expanded form is

$$\begin{aligned}(\psi_{x_I})_{i,j,k} = \frac{1}{2h}\Bigg[&\frac{16}{36}\left(\psi_{i+1,j,k} - \psi_{i-1,j,k}\right) + \frac{4}{36}\left(\{\psi_{i+1,j,k+1} + \psi_{i+1,j,k-1} + \psi_{i+1,j+1,k} + \psi_{i+1,j-1,k}\}\right.\\ &\left. - \{\psi_{i-1,j,k+1} + \psi_{i-1,j,k-1} + \psi_{i-1,j+1,k} + \psi_{i-1,j-1,k}\}\right)\\ &+ \frac{1}{36}\left(\{\psi_{i+1,j+1,k+1} + \psi_{i+1,j-1,k+1} + \psi_{i+1,j+1,k-1} + \psi_{i+1,j-1,k-1}\}\right.\\ &\left. - \{\psi_{i-1,j+1,k+1} + \psi_{i-1,j-1,k+1} + \psi_{i-1,j+1,k-1} + \psi_{i-1,j-1,k-1}\}\right)\Bigg].\end{aligned}$$

Similarly, isotropic finite difference of ψ_{xx} is obtained from

$$(\psi_{xx_I})_{i,j,k} = \left(1 + \frac{h^2}{12}\nabla^2\right)(\psi_{xx})_{i,j,k}.$$

The above, to $\mathcal{O}(h^2)$, is expressed as

$$(\psi_{xx_I})_{i,j,k} = \left(1 + \frac{h^2}{12}\eth_{zz}\right)\left(1 + \frac{h^2}{12}\eth_{yy}\right)(\psi_{xx_C})_{i,j,k},$$

which in expanded form is

$$\begin{aligned}(\psi_{xx_I})_{i,j,k} = \frac{1}{h^2}\Bigg[&\frac{100}{144}\left(\psi_{i+1,j,k} - 2\psi_{i,j,k} + \psi_{i-1,j,k}\right) + \frac{10}{144}\left(\{\psi_{i+1,j,k+1} + \psi_{i+1,j,k-1} + \psi_{i+1,j+1,k} + \psi_{i+1,j-1,k}\}\right.\\ &\left. - 2\{\psi_{i,j,k+1} + \psi_{i,j,k-1} + \psi_{i,j+1,k} + \psi_{i,j-1,k}\} + \{\psi_{i-1,j,k+1} + \psi_{i-1,j,k-1} + \psi_{i-1,j+1,k} + \psi_{i-1,j-1,k}\}\right)\\ &+ \frac{1}{144}\left(\{\psi_{i+1,j+1,k+1} + \psi_{i+1,j-1,k+1} + \psi_{i+1,j+1,k-1} + \psi_{i+1,j-1,k-1}\} - 2\{\psi_{i,j+1,k+1} + \psi_{i,j-1,k+1}\right.\\ &\left. + \psi_{i,j+1,k-1} + \psi_{i,j-1,k-1}\} - \{\psi_{i-1,j+1,k+1} + \psi_{i-1,j-1,k+1} + \psi_{i-1,j+1,k-1} + \psi_{i-1,j-1,k-1}\}\right)\Bigg].\end{aligned}$$

Conventional finite difference of ψ_{xy} is obtained from

$$(\psi_{xy_C})_{i,j,k} = \frac{1}{4h^2}\left(\psi_{i+1,j+1,k} - \psi_{i-1,j+1,k} - \psi_{i+1,j-1,k} + \psi_{i-1,j-1,k}\right),$$

which to $\mathcal{O}(h^2)$ gives

$$(\psi_{xy_C})_{i,j,k} = \left(1 + \frac{h^2}{6}\{\delta_{xx} + \delta_{yy}\}\right)(\psi_{xy})_{i,j,k}.$$

Isotropic finite difference of ψ_{xy} is obtained from

$$(\psi_{xy_I})_{i,j,k} = \left(1 + \frac{h^2}{6}\nabla^2\right)(\psi_{xy})_{i,j,k}.$$

The above is expressed as

$$(\psi_{xy_I})_{i,j,k} = \left(1 + \frac{h^2}{6}\delta_{zz}\right)(\psi_{xy_C})_{i,j,k},$$

which in expanded form is

$$\begin{aligned}(\psi_{xy_I})_{i,j,k} = \frac{1}{4h^2}\Bigg[&\frac{1}{6}\{\psi_{i+1,j+1,k+1} - \psi_{i-1,j+1,k+1} - \psi_{i+1,j-1,k+1} + \psi_{i-1,j-1,k+1}\}\\ &+\frac{4}{6}\{\psi_{i+1,j+1,k} - \psi_{i-1,j+1,k} - \psi_{i+1,j-1,k} + \psi_{i-1,j-1,k}\}\\ &+\frac{1}{6}\{\psi_{i+1,j+1,k-1} - \psi_{i-1,j+1,k-1} - \psi_{i+1,j-1,k-1} + \psi_{i-1,j-1,k-1}\}\Bigg].\end{aligned}$$

An isotropic discretisation of the Laplacian can be obtained by combining the isotropic formulae for the second derivatives

$$(\nabla_I^2\psi)_{i,j,k} = \frac{1}{48h^2}\left(20\sum_{NN}\psi + 6\sum_{NNN}\psi + \sum_{NNNN}\psi - 200\psi\right)_{i,j,k},$$

where *NN* refers to the nearest-neighbour points, *NNN* to the next-nearest-neighbour points, and *NNNN* to the next-next-nearest-neighbour points.

We once again note that the stability criterion for the heat conduction equation, which is $\Delta t/h^2 \leqslant 1/6$ when the conventional central differences are used, is enhanced to $\Delta t/h^2 \leqslant 3/8$ when the isotropic discretisation of the three-dimensional Laplacian is used.

Appendix B. ADI scheme

ADI scheme used in the present work is described. Consider the PDE

$$\frac{\partial U}{\partial t} = a_{11}U_{xx} + a_{22}U_{yy} - r.$$

Let U^n be the solution at $t = t_n$. Using the ADI scheme the solution is advanced from t_n to t_{n+1} in two steps, from t_n to $t_{n+\frac{1}{2}}$, and from $t_{n+\frac{1}{2}}$ to t_{n+1}. The integration from t_n to $t_{n+\frac{1}{2}}$ is carried out as follows:

$$\frac{U^{n+\frac{1}{2}}-U^{n}}{\frac{1}{2}\Delta t}=a_{11}^{n+\frac{1}{2}}U_{xx}^{n+\frac{1}{2}}+a_{22}^{n}U_{yy}^{n}-r^{n+\frac{1}{2}}.$$

We define $U^{n+\frac{1}{2},m}$ as the mth iterate of $U^{n+\frac{1}{2}}$. We solve the above equation as

$$\frac{2}{\Delta t}\left(U^{n+\frac{1}{2},m+1}-U^{n}\right)=a_{11}^{n+\frac{1}{2},m}U_{xx}^{n+\frac{1}{2},m+1}+a_{22}^{n}U_{yy}^{n}-r^{n+\frac{1}{2},m}.$$

Let $\delta=U^{n+\frac{1}{2},m+1}-U^{n+\frac{1}{2},m}$. δ is then obtained from

$$\left(a_{11}^{n+\frac{1}{2},m}\delta_{xx}\right)-\frac{2}{\Delta t}\delta=-\left(a_{11}^{n+\frac{1}{2},m}U_{xx}^{n+\frac{1}{2},m}-r^{n+\frac{1}{2},m}\right)-\left(a_{22}^{n}U_{yy}^{n}\right)+\frac{2}{\Delta t}\left(U^{n+\frac{1}{2},m}-U^{n}\right).$$

The above equation is solved as the tridiagonal system for each j. The left hand side of the tridiagonal system can be written as

$$\left(c_{21}a_{11}^{n+\frac{1}{2},m}\right)\delta_{i-1,j}+\left(c_{20}a_{11}^{n+\frac{1}{2},m}-\frac{2}{\Delta t}\right)\delta_{i,j}+\left(c_{21}a_{11}^{n+\frac{1}{2},m}\right)\delta_{i+1,j}=(\mathrm{RHS})_{i,j},$$

where *RHS* stands for the right hand side. We take $c_{21}=1/h^2$, and $c_{20}=-2/h^2$ for the conventional scheme, and $c_{21}=10/(12h^2)$, and $c_{20}=-20/(12h^2)$ for the isotropic scheme, and the solution is iterated (note m) until a prescribed convergence. Δt is decreased if the iterations do not converge within a prescribed $m_{\max}$.

In the integration from $t_{n+\frac{1}{2}}$ to t_{n+1} the following equation along j-direction is considered

$$\left(a_{22}^{n+1,m}\delta_{yy}^{*}\right)-\frac{2}{\Delta t}\delta^{*}=-\left(a_{22}^{n+1,m}U_{yy}^{n+1,m}-r^{n+1,m}\right)-\left(a_{11}^{n+\frac{1}{2}}U_{xx}^{n+\frac{1}{2}}\right)+\frac{2}{\Delta t}\left(U^{n+1,m}-U^{n+\frac{1}{2}}\right),$$

where $\delta^{*}=U^{n+1,m+1}-U^{n+1,m}$. Steps similar to going from t_n to $t_{n+\frac{1}{2}}$ are followed.

References

[1] J.S. Langer, Instabilities and pattern formation in crystal growth, Rev. Mod. Phys. 52 (1980) 1–28.

[2] A. Karma, W.-J. Rappel, Phase-field method for computationally efficient modelling of solidification with arbitrary interface kinetics, Phys. Rev. E 53 (1996) R3017–R3020.

[3] R.J. Braun, B.T. Murray, Adaptive phase-field computations of dendritic crystal growth, J. Cryst. Growth 174 (1997) 41–53.

[4] Y.-T. Kim, N. Provatas, N. Goldenfeld, J. Dantzig, Universal dynamics of phase-field models for dendritic growth, Phys. Rev. E 59 (1999) R2546–R2549.

[5] L. Granasy, T. Pusztai, J.A. Warren, J.F. Douglas, T. Borzsonyi, V. Ferreiro, Growth of dizzy dendrites in a random field of foreign particles, Nat. Mat. 2 (2003) 92–96.

[6] L. Collatz, The numerical treatment of differential equation, Springer-Verlag, Berlin, 1966;
G. Dahlquist, A. Bjorck, Numerical methods, Prentice Hall, Englewood Cliffs, NJ, 1974.

[7] D. Barkley, M. Kness, L.S. Tuckerman, Spiral wave dynamics in a simple model of excitable media: the transition from simple to compound rotation, Phys. Rev. A 42 (1990) 2489–2492.